Renewable Energy 33 (2008) 2559–2572

Contents lists available at ScienceDirect

Renewable Energy

journal homepage: www.elsevier.com/locate/renene

Multi-objective design of PV–wind–diesel–hydrogen–battery systems

Rodolfo Dufo-López, José L. Bernal-Agustín *

Department of Electrical Engineering, University of Zaragoza, Calle María de Luna 3, 50018-Zaragoza, Spain

A R T I C L E I N F O

Article history:
Received 20 July 2007
Accepted 19 February 2008
Available online 9 April 2008

Keywords:
Hybrid systems
Multi-objective design
Multi-objective evolutionary algorithms
Genetic algorithms

A B S T R A C T

This paper presents, for the first time, a triple multi-objective design of isolated hybrid systems minimizing, simultaneously, the total cost throughout the useful life of the installation, pollutant emissions (CO_2) and unmet load.

For this task, a multi-objective evolutionary algorithm (MOEA) and a genetic algorithm (GA) have been used in order to find the best combination of components of the hybrid system and control strategies.

As an example of application, a complex PV–wind–diesel–hydrogen–battery system has been designed, obtaining a set of possible solutions (Pareto Set).

The results achieved demonstrate the practical utility of the developed design method.

1. Introduction

When carrying out a design taking into account several objectives simultaneously, it is typical that some of them are in conflict with some others [1].

This paper shows the design of a hybrid PV–wind–diesel–hydrogen–battery installation for the generation of electric energy (Fig. 1, wind turbines could be connected either at DC bus, as shown in the figure, or at AC bus), considering simultaneously three objectives (cost, pollutant emissions, and unmet load) which are usually in conflict, since when one of them gets improved, the others get worse. The design of a hybrid system, considering the three mentioned objectives, poses a very complex problem of optimization.

In the specialized technical literature [2–8], the design of these systems is usually done by searching the configuration and/or control that renders the lowest total cost throughout the useful life of the installation, considering a fixed value for the unmet load, previously decided by the designer, and in some cases, the pollutant emissions are also limited or economically evaluated.

Therefore, the result obtained will depend on the unmet load value selected, on the limitation of the pollutant emissions and/or on the subjective assignation of costs to the pollutant emissions. Using these techniques, the solutions can be very far from the global optimum.

However, some multi-objective design methods already exist and they have been applied successfully in several fields of engineering [1]. Given the complexity of this kind of problems, because of the large number of variables that are usually considered and of the mathematical models applied, classical optimization techniques may consume excessive CPU time or even be unable to take into account all the characteristics associated to the posed problem.

Because of this, during the last 3 decades, heuristic techniques have been applied [9]. One of the most used heuristic techniques has been the multi-objective evolutionary algorithms (MOEAs). MOEA's stand out for this task, being applied in numerous research works [10].

One of the most important characteristics of this kind of algorithms is the concept of Pareto Optimality [10]; thanks to it, as a result of the optimization process, a set of possible solutions is obtained after a searching process in which the objectives involved in the design are evaluated independently. From the obtained solutions, the designer can choose those that he/she thinks to be more appropriate depending on the values of the objectives considered.

From the MOEAs developed until now, the 'state of the art' [10] about this subject indicates that the strength Pareto evolutionary algorithm (SPEA, SPEA2) [11,12] is not only one of the most efficient algorithms but also the one that gives the best results. Because of this, in the study explained in this paper, the SPEA is applied to the multi-objective design of hybrid systems.

In a previous work, the authors showed the optimization of multi-objective design of isolated hybrid systems minimizing the total cost throughout the useful life of the installation and the pollutant emissions (CO_2) [13].

This paper starts by showing the mathematical model of the components, followed by the description of the objective functions and the basic concepts related to the problems of

* Corresponding author. Tel.: +34 976 76 19 21; fax: +34 976 76 22 26.
E-mail addresses: rdufo@unizar.es (R. Dufo-López), jlbernal@unizar.es (J.L. Bernal-Agustín).

0960-1481/$ - see front matter
doi:10.1016/j.renene.2008.02.027

Nomenclature

a integer that matches the code that identifies the number of PV panels in parallel (or PV generators in parallel)
A_E coefficient of the electrolyzer electricity consumption curve (kW/kg/h)
A_{FC} coefficient of the fuel cell hydrogen consumption curve (kg/kWh)
A_G coefficient of the diesel generator fuel consumption curve (l/kWh)
b integer that matches the code that identifies a certain type of PV panel or PV generator
B_E coefficient of the electrolyzer electricity consumption curve (kW/kg/h)
B_{FC} coefficient of the fuel cell hydrogen consumption curve (kg/kWh)
B_G coefficient of the Diesel generator fuel consumption curve (l/kWh)
c integer that matches the code which identifies a certain wind turbine model
$\cos\varphi$ power factor of the AC load
CF cycles to failure
CF_i number of cycles to failure of the battery in the interval DOD_i
$Cons_E$ electrical energy consumption of the electrolyzer (kW)
$Cons_{FC}$ hydrogen consumption of the fuel cell (kg/h)
$Cons_G$ fuel consumption of the diesel generator (l/h)
d integer that matches the code that identifies the number of wind turbines
DOD depth of discharge of the battery (%)
DOD_i interval between two values of DOD
e integer that matches the code which identifies a certain hydro turbine model
E total amount of kg of CO_2 produced by the hybrid system throughout 1 year (kg/year)
f integer that matches the code that identifies the number of batteries in parallel (or groups of batteries banks in parallel)
F_{ef} fuel cell consumption factor to consider the high consumption above P_{max_ef}
$fitness_{main}$ fitness of a solution of the main algorithm (combination of components)
$fitness_{sec}$ fitness of a solution of the secondary algorithm (control strategy)
F_{loss} factor that takes into account the losses of power given by the PV panels due to shadows, dirt, etc.
g integer that matches the code that identifies a certain type of battery or batteries bank
GA genetic algorithm
h integer that indicates the code that matches the size of the AC generator (diesel usually) used in the system
H_2TANK_{stp} setpoint for the amount of H_2 stored in the tank, value optimized by the program (kg)
HHV_{H_2} higher heating value of hydrogen (39.3 kWh/kg)
i integer that matches the code that identifies a certain fuel cell
j integer that matches the code that identifies a certain electrolyzer
k integer that matches the code that identifies a certain inverter
$LHV_{GAS-OIL}$ lower heating value of gas–oil (kWh/l)
LHV_{H_2} lower heating value of hydrogen (33.3 kWh/kg)
MOEA multi-objective evolutionary algorithm
N_i number of cycles of the battery in the interval DOD_i in 1 year
N_{max} maximum size allowed of the Pareto Set (non-dominated solutions)
N_{gen_main} number of generations of the main algorithm
$N_{gen\_main\_max}$ maximum number of generations of the main algorithm
N_{gen_sec} number of generations of the secondary algorithm
$N_{gen\_sec\_max}$ maximum number of generations of the secondary algorithm
N_m population of the main algorithm: number of solutions (vectors) of the main algorithm
N_{non_dom} number of non-dominated solutions
NPC net present cost of the system (€)
NPC_{over} maximum NPC for the non-dominated solutions, in percentage over the minimum NPC of the non-dominated solutions (%)
N_{sec} population of the secondary algorithm: number of solutions (vectors) of the secondary algorithm
$P_{critical\_gen}$ power under which the diesel generator, instead of providing exactly the necessary value required to satisfy demand, provides the nominal power (or the possible maximum without losing energy), using the surplus energy to charge the batteries until a certain level of charge called SOC_{stp_gen} (W)
P_{FC} output power of the fuel cell (kW)
P_G output power of the AC generator (kW)
P_{lim_disch} discharge limit power (W)
P_{max_ef} fuel cell output power that has the maximum efficiency (% of P_{N_FC}) (%)
P_{min_gen} minimum operational power of the diesel generator optimized by the program (W)
P_{min_FC} minimum operational power of the fuel cell optimized by the program (W)
P_{N_FC} nominal power of the fuel cell (kW)
P_{N_G} nominal power of the diesel generator (kW)
$P_{re\_pv\_i}$ power supplied by the PV panels, during the hour i (W)
$P_{re\_w\_i}$ power supplied by the wind tubine, during the hour i (W)
$P1_{FC}$ intersection point of the cost of supplying energy with the batteries and the cost of supplying energy with the fuel cell. Value optimized by the program (W)
$P1_{gen}$ intersection point of the cost of supplying energy with the batteries and the cost of supplying energy with the AC generator. Value optimized by the program (W)
P2 intersection point of the cost of supplying energy with the fuel cell and the cost of supplying energy with the AC generator. Value optimized by the program (W)
Q_{N_E} electrolyzer hydrogen mass flow (kg/h)
Q_{N_E} electrolyzer nominal hydrogen mass flow (kg/h)
SOC state of charge of the batteries (% of C_N)
SOC_{min} minimum state of charge of the battery bank (% of nominal capacity)
SOC_{stp_gen} SOC set point of the batteries (% of nominal capacity)
SPEA strength Pareto evolutionary algorithm
UL annual unmet load (kWh/year)
UL (%) unmet load as a percentage of the overall load (%)
v_{hub_i} wind speed at the hub height of the wind turbine, during the hour i (m/s)

v_{data_i}	wind speed at anemometer height, during the hour i (m/s)
z_0	the surface roughness length (m)
z_{data}	the anemometer height (m). This is the height in which the wind data has been read
z_{hub}	the hub height of the wind turbine (m)
$\eta_{E\%}$	electrolyzer efficiency (in % of the higher heating value of hydrogen, HHV_{H_2}) (%)
$\eta_{FC\%}$	fuel cell efficiency (in % of the lower heating value of hydrogen, LHV_{H_2}) (%)
η_G	diesel generator efficiency (kWh/l)
$\eta_{G\%}$	diesel generator efficiency (in % of the lower heating value of gas–oil, $LHV_{GAS-OIL}$) (%)

multi-objective optimization and the evolutionary algorithms applied to it. Finally, the results and conclusions obtained from the multi-objective design of a PV–wind–diesel–hydrogen–battery system are shown, thus verifying the good behavior of the SPEA as a design tool.

2. Mathematical model of the components

A more detailed mathematical model of the components of the hybrid system (PV panels, wind turbines, diesel generator, electrolyzer, fuel cell, hydrogen tank, and batteries) and the control strategy can be found in previous works [7,13–15]. A brief description of such mathematical models is shown in forthcoming subsections.

2.1. Current from the PV generator

The input data could be the monthly average daily radiation on the horizontal surface or the peak sun hours. Using the Rietveld equation [16], the design tool converts the input data into the average clearness index for each month of the year, obtaining the clearness index for each day of the year and calculating the global hourly irradiation G (kWh/m^2) according to the Graham model [17].

Alternatively, hourly irradiation data can be read from a file in which the global irradiation on horizontal surface for each hour of the year and for the geographic place of the design are included.

The power supplied by the panels, during the hour i, is calculated by Eq. (1):

$$P_{re\_pv\_i} = G_i \times I_{sc} \times F_{loss} \times U_{DC}, \quad (1)$$

where I_{sc} is the shortcut current of the PV generator, F_{loss} is the factor that takes into account the losses of power given by the PV panels due to shadows, dirt, etc., and U_{DC} is the DC voltage.

2.2. Batteries

The design tool allows calculating the charge condition of the batteries and the maximum admissible current by using two different models: The Ah model [18] or the KiBaM model [19].

On the other side, there are several models to predict the expected lifespan of batteries [20], which depends on the conditions of operation, on the charge/discharge regime and on temperature. Calculating the expected lifespan of batteries is important, as it influences the total cost of the system.

With this design tool, it is possible to choose between two different methods in order to estimate the lifespan of batteries:

- The first alternative is to estimate it through cycles to failure, (HOMER program [21] uses this method), considering, in this case, that the battery lifespan depends on the depth of discharge (DOD) of the charge/discharge cycles, as seen in Fig. 2. Applying this method, it is possible to define the equivalent full cycles as the number of cycles to failure multiplied by the DOD. The average of equivalent full cycles will be the value used to calculate the life of batteries.
- The other method—which can also be applied using the design tool shown in this paper—for estimating battery lifespan is more complex and precise; it is the cycles counting method known as "rainflow", based on Downing's algorithm [22], which is used by the HYBRID2 program [23]. The method of cycles counting is based on counting the charge/discharge cycles. The number of cycles corresponding to each range of

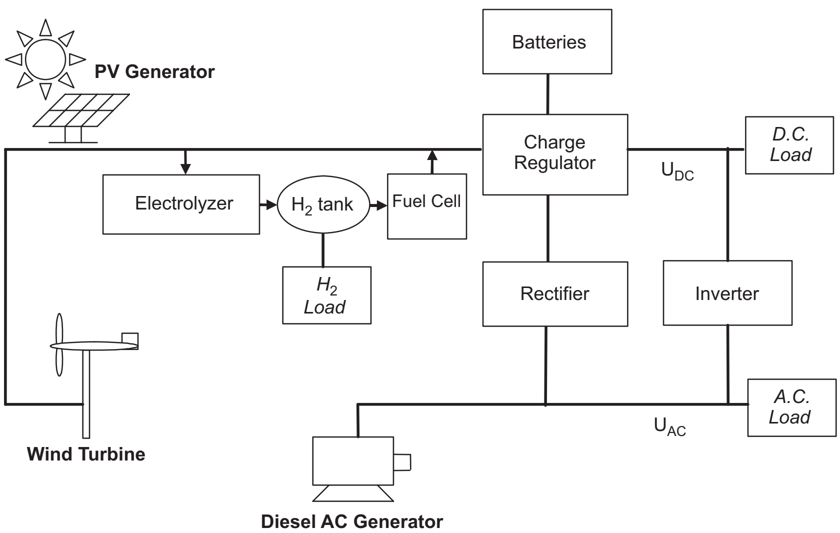

Fig. 1. PV–wind–diesel–hydrogen–battery system.

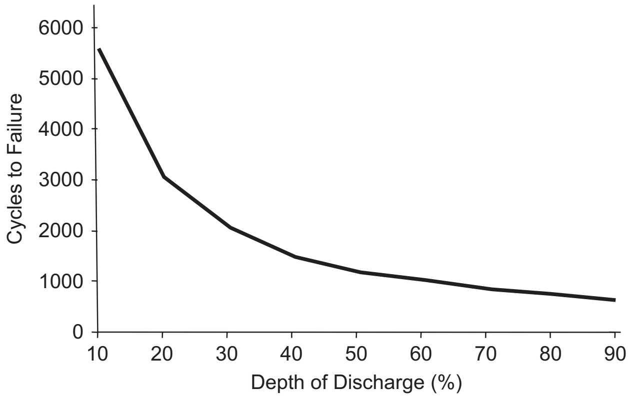

Fig. 2. Battery cycles to failure vs. depth of discharge.

the DOD (split in m intervals) for 1 year is counted. For example, breaking up the DOD in 10 intervals, N_1 will be the number of cycles between 0% and 10% of the DOD, N_2 will be the number of cycles between 10% and 20% of the DOD, etc. For each interval, there will be a number of cycles to failure (CF_i) obtained from Fig. 2. Battery duration, in years, can be calculated using Eq. (2):

$$\mathrm{Life}_{\mathrm{bat}} = \frac{1}{\sum_{i=1}^{m} (N_i/\mathrm{CF}_i)}. \tag{2}$$

2.3. Current from the wind turbine

To estimate the current generated by the wind turbine, the design tool uses the power curves supplied by the manufacturer for each wind turbine [24].

Besides, it is necessary to know the hourly values of the wind, which are read from a file in which is included the wind speed for each hour of the year and for the geographic place where the design is carried out. To calculate the output of the wind turbine in each of the 8760 h, the applied methodology is briefly described as follows [24].

The method has two steps:

- *First*. The hourly wind speed at the hub height is calculated by using Eq. (3):

$$v_{\mathrm{hub}\_i} = v_{\mathrm{data}\_i} \frac{\ln(z_{\mathrm{hub}}/z_0)}{\ln(z_{\mathrm{data}}/z_0)}, \tag{3}$$

  where z_{hub} is the hub height of the wind turbine (m), z_{data} is the anemometer height (m). This is the height in which the wind data has been read. z_0 is the surface roughness length (m), v_{hub_i} is wind speed at the hub height of the wind turbine, during the hour i (m/s), v_{data_i} is wind speed at anemometer height, during the hour i (m/s).
- *Second*. Using the power curve of the wind turbine, the power output is calculated. With the speed at the hub of the wind turbine, and using its power curve, it is obtained by the power that the wind turbine provides in hour i, $P_{\mathrm{re\_w}\_i}$.

2.4. Inverter

The inverter has been modeled in a realistic way, considering the efficiency variable as a function of apparent power output (% of rated apparent power in VA).

2.5. Diesel generator fuel consumption

The fuel consumption of the diesel generator, $\mathrm{Cons}_{\mathrm{G}}$ (l/h) is modeled as dependent on the output power:

$$\mathrm{Cons}_{\mathrm{G}} = B_{\mathrm{G}} \times P_{\mathrm{N\_G}} + A_{\mathrm{G}} \times P_{\mathrm{G}}, \tag{4}$$

where $P_{\mathrm{N\_G}}$ (kW) is the nominal power, P_{G} (kW) is the output power of the diesel generator, A_{G} and B_{G} are the coefficients of the consumption curve, defined by the user (l/kWh).

The efficiency η_{G} (kWh/l) is calculated using Eq. (5):

$$\eta_{\mathrm{G}} = \frac{P}{\mathrm{Cons}_{\mathrm{G}}} = \frac{1}{A_{\mathrm{G}} + B_{\mathrm{G}} \times P_{\mathrm{N\_G}}/P}. \tag{5}$$

The efficiency in % of the lower heating value (LHV) of gas–oil ($\eta_{\mathrm{G\%}}$ (%)) is calculated from Eq. (6):

$$\eta_{\mathrm{G\%}} = \frac{\eta_{\mathrm{G}}\ (\mathrm{kWh/l})}{\mathrm{LHV}_{\mathrm{GAS-OIL}}\ (\mathrm{kWh/l})} \times 100 = \frac{100 \times P}{\mathrm{Cons}_{\mathrm{G}} \times \mathrm{LHV}_{\mathrm{GAS-OIL}}}, \tag{6}$$

where $\mathrm{LHV}_{\mathrm{GAS-OIL}}$ is between 10 and 11.6 kWh/l. In this work, it is considered $\mathrm{LHV}_{\mathrm{GAS-OIL}} = 11.55$ kWh/l. Skarstein and Ulhen [25] proposed $A_{\mathrm{G}} = 0.246$ l/kWh and $B_{\mathrm{G}} = 0.08145$ l/kWh. The efficiency (% of $\mathrm{LHV}_{\mathrm{GAS-OIL}}$) in this case is 26.4% at rated power.

2.6. Fuel cell hydrogen consumption

The hydrogen consumption of the fuel cell, $\mathrm{Cons}_{\mathrm{FC}}$ (kg/h) is modeled as dependent on the output power:

If $P/P_{\mathrm{N\_FC}} \leqslant P_{\mathrm{max\_ef}}$:

$$\mathrm{Cons}_{\mathrm{FC}} = B_{\mathrm{FC}} \times P_{\mathrm{N\_FC}} + A_{\mathrm{FC}} \times P_{\mathrm{FC}}. \tag{7}$$

If $P/P_{\mathrm{N\_FC}} > P_{\mathrm{max\_ef}}$:

$$\mathrm{Cons}_{\mathrm{FC}} = B_{\mathrm{FC}} \times P_{\mathrm{N\_FC}} + A_{\mathrm{FC}} \times P_{\mathrm{FC}} \left(1 + F_{\mathrm{ef}} \left(\frac{P}{P_{\mathrm{N\_FC}}} - P_{\mathrm{max\_ef}}\right)\right), \tag{8}$$

where P_{FC} is the output power (kW), $P_{\mathrm{N\_FC}}$ (kW) is the nominal output power, A_{FC} and B_{FC} are the coefficients of the consumption curve (kg/kWh), $P_{\mathrm{max\_ef}}$ (% of $P_{\mathrm{N\_FC}}$) is the output power that has the maximum efficiency and F_{ef} is the factor to consider the high consumption above $P_{\mathrm{max\_ef}}$.

The efficiency in % of the LHV of hydrogen ($\mathrm{LHV}_{\mathrm{H_2}}$) is calculated using Eq. (9):

$$\eta_{\mathrm{FC\%}} = \frac{100 \times P}{\mathrm{Cons}_{\mathrm{FC}} \times \mathrm{LHV}_{\mathrm{H_2}}}, \tag{9}$$

where $\mathrm{LHV}_{\mathrm{H_2}} = 33.3$ kWh/kg. The hydrogen consumption parameters considered in Section 5 are the same for all the fuel cells (they are defined by the user): $A_{\mathrm{FC}} = 0.05$ kg/kWh, $B_{\mathrm{FC}} = 0.004$ kg/kWh, $P_{\mathrm{max\_ef}} = 0.2$ and $F_{\mathrm{ef}} = 1$. The efficiency corresponding to these values has a maximum value of 46% and a value of 31% at rated power.

2.7. Electrolyzer electrical consumption

The electrical consumption ($\mathrm{Cons}_{\mathrm{E}}$ (kW)) is modeled as dependent on the hydrogen mass flow:

$$\mathrm{Cons}_{\mathrm{E}} = B_{\mathrm{E}} \times Q_{\mathrm{N\_E}} + A_{\mathrm{E}} \times Q, \tag{10}$$

where $Q_{\mathrm{N\_E}}$ is the nominal hydrogen mass flow (kg/h), Q is the hydrogen mass flow (kg/h), A_{E} and B_{E} are the coefficients of the consumption curve (kW/kg/h).

The efficiency in % of the higher heating value of hydrogen ($\mathrm{HHV}_{\mathrm{H_2}}$) is calculated using Eq. (11):

$$\eta_{\mathrm{E\%}} = \frac{100 \times Q \times \mathrm{HHV}_{\mathrm{H_2}}}{\mathrm{Cons}_{\mathrm{E}}}, \tag{11}$$

where $HHV_{H_2} = 39.4$ kWh/kg. The electrical consumption parameters considered in Section 5 of this work are the same for all the electrolyzers (they are defined by the user): $A_E = 40$ kW/kg/h, $B_E = 20$ kW/kg/h. The efficiency (% of higher heating value of hydrogen) corresponding to these values presents a maximum value of 65.6% at rated power.

3. Objective functions

The objective functions to be minimized are:

- The total net present cost: NPC (€).
- The CO_2 emissions: E (kg/year).
- The unmet load: UL (kWh/year).

3.1. Costs

The costs objective function is the total net present cost of the system (NPC), which includes the cost of the initial investment plus the discounted present values of all future costs throughout the total life of the installation. The life of the system is usually considered to be the life of the PV panels, which are the elements that have a longer lifespan.

In the following paragraph, the costs taken into account are indicated. A more detailed description of its calculation can be found in Refs. [7,13–15].

- Cost for purchasing the PV panels, the wind turbine, the batteries, the inverter, the charge regulator, the diesel generator, the electrolyzer, the fuel cell, and the hydrogen tank.
- Costs of maintenance of the components.
- Costs of replacing the components throughout the life of the system.
- Costs of operation and maintenance of components throughout the life of the system.
- Cost of the fuel consumed throughout the life of the system.

Some of the costs depend on the control strategy selected amongst those possible [7,14,15].

It has been considered that at the end of the life of the system, the remaining value of the elements is recovered.

3.2. Pollutant emissions

In order to measure the pollutant emissions, kg of CO_2 is considered; it represents the largest percentage of all emissions when fuel is burnt [26], and it is the main cause of the greenhouse effect. It is considered that the total amount of kg of CO_2 produced by the hybrid system throughout 1 year (E) is the correct measure of the pollutant emissions and, therefore, it can be used as the objective to be minimized.

The developed algorithm has as input data the number of kg of CO_2 produced per litre of fuel consumed by the diesel generator. This value depends upon the characteristics of the diesel generator and of the characteristics of the fuel, and it usually falls in the 2.4–2.8 kg/l range [26].

3.3. Unmet load

The unmet load (UL) is defined as the amount of non-served energy in 1 year, and it is usually measured in kWh/year. In percentage, it can be defined as follows:

$$\mathrm{UL}\,(\%) = \frac{\mathrm{UL}\,(\mathrm{kWh/year})}{\mathrm{Total\ annual\ electrical\ load}\,(\mathrm{kWh/year})} \times 100. \tag{12}$$

The maximum unmet load allowed is an input of the developed design tool.

The possible solutions (combinations of elements of the system and control strategies) that give a rate of unmet load higher than the maximum allowed by the user are discarded.

4. Multi-objective optimization evolutionary algorithm

In this section, the multi-objective design problem is mathematically formulated, and the basic concepts used by the MOEAs are defined.

Finally, it is also described the applied MOEA (SPEA), that searches the best combination of components minimizing NPC, pollutant emissions and unmet load. The design tool also uses a genetic algorithm (GA) to find the best control for each combination of components, and it is also described.

4.1. Concepts related to multi-objective optimization problems

A multi-objective optimization problem can be defined as follows [9]:

- Minimize or maximize the objective functions included in the vector:

$$F(x) = [f_1(x), f_2(x), \ldots, f_k(x)]. \tag{13}$$

- Satisfying the m restrictions of inequality and the p restrictions of equality:

$$\begin{aligned} g_i(x) &\geqslant 0, \quad i = 1, 2, \ldots, m \\ h_i(x) &= 0, \quad i = 1, 2, \ldots, p \end{aligned} \tag{14}$$

where x is a vector whose elements are the decisive variables of the problem.

Concepts related to Pareto optimality are regularly used in most MOEAs. Because of this, the concepts of Pareto dominance, Pareto optimality, Pareto optimal set and Pareto front are defined, as they appear in Ref. [10].

- Pareto dominance: a vector $u = (u_1, u_2, \ldots, u_k)$ is said to dominate $v = (v_1, v_2, \ldots, v_k)$ (denoted by $u \preceq v$) if and only if u is partially less than v, i.e., $\forall i \in \{1, 2, \ldots, k\}$, $u_i \preceq \npreceq v_i \wedge \exists i \in \{1, 2, \ldots, k\}$: $u_i < v_i$.
- Pareto optimality: a solution $x \in \Omega$ is said to be Pareto optimal with respect to Ω if and only if there is no $x' \in \Omega$ for which $v = F(x') = (f_1(x'), f_2(x'), \ldots, f_k(x'))$ dominates $u = F(x) = (f_1(x), f_2(x), \ldots, f_k(x))$.
- Pareto optimal set: for a given MOP $F(x)$, the Pareto optimal set (P^*) is defined as follows:

$$P^* = \{x \in \Omega \mid \neg \exists x' \in \Omega : F(x') \preccurlyeq F(x)\}. \tag{15}$$

- Pareto front: for a given MOP $F(x)$ and Pareto optimal set P^*, the Pareto front (PF^*) is defined as follows:

$$PF^* = \{u = F(x) = (f_1(x), f_2(x), \ldots, f_k(x)) \mid x \in P^*\}. \tag{16}$$

4.2. MOEA applied to the design of PV–wind–diesel–hydrogen–battery systems

The implemented multi-objective algorithm is based on SPEA and SPEA2 [11,12]. This algorithm is in charge of finding the designs that manage to, simultaneously, minimize the NPC of the system, the pollutant emissions (E) and the unmet load (UL). It has been developed using the C# programming language.

The characteristics of the MOEA that has been applied in this study are described as follows.

4.2.1. Codification of solutions

The program uses two different evolutionary algorithms. The main algorithm is the MOEA algorithm and codifies the components of the system. The secondary algorithm is a GA that codifies the control strategy. For each combination of components in the main algorithm (multi-objective), the secondary algorithm (mono-objective) runs to find its best control strategy (lowest NPC).

4.2.2. Main algorithm (MOEA)

The main algorithm (MOEA) can search for the configuration of PV panels, wind generators, hydro turbine, batteries, AC generator, fuel cell, electrolyzer, and inverter that minimizes the three objectives mentioned. This is the general case, if all these elements are selected [14,15]. However, in the computational results presented in this paper, the system contains only some of these elements (PV–wind–diesel–hydrogen–batteries system).

In the general case, the codification of the variables used by the main algorithm is done through a vector made up of 11 integers:

$$|a|b|c|d|e|f|g|h|i|j|k|, \qquad (17)$$

where, a is the number of PV panels in parallel, b is the type of PV panel, c is the number of wind turbines, d is the type of wind turbine, e is the type of hydro turbine, f is the number of batteries in parallel, g is the type of battery, h is the type of AC generator (usually diesel), i is the type of fuel cell, j is the type of electrolyzer, k is the type of inverter.

Regarding the inverter, it can be forced to supply the maximum power demanded by the AC load, which is an option of the design tool. In this case, the inverter selected will be the one with the lowest power whose output is higher than the AC load maximum. If this option is not used, the type of inverter will be a variable to be optimized, being possible that an inverter whose output is bigger than the maximum AC consumption is not needed; in this case, higher net load will be supplied by the AC generator.

The charge regulator, the battery charger and the H_2 tank do not take part in the combination of components optimized by the main algorithm. This is so because, for each possible combination calculated by the main algorithm, the optimal size of these components is determined once the secondary algorithm has obtained the best control strategy.

The fitness function of the combination i of the main algorithm is assigned according to its rank in the population. The rank is obtained sorting the solutions out according to the number of solutions by which they are dominated: first, the non-dominated solutions (dominated by cero solutions), then the dominated by one solution, then the dominated by two solutions, and so on.

The solutions that are dominated by the same number of solutions must have the same fitness, which will be the average fitness of these solutions. All the non-dominated solutions must have the same fitness, all the solutions dominated by 1 must have the same fitness, and so on:

$$\mathrm{fitness}_{\mathrm{MAIN}_i} = \frac{\sum_k \left[(N_\mathrm{m}+1) - i / \sum_j [(N_\mathrm{m}+1) - j] \right]}{b - a + 1}, \qquad (18)$$

where N_m is the number of solutions of the main algorithm, i is the rank of the solution of which it is calculated its fitness, j are all the solutions of the main algorithm ($j = 1, \ldots, N_\mathrm{m}$), k are all the solutions dominated by the same number of solutions as the solution i ($k = a, \ldots, b$).

4.2.3. Secondary algorithm (GA)

There are 12 control variables of the hybrid system and all of them are optimized by the secondary GA: $P_{\mathrm{min\_gen}}$, $P_{\mathrm{min\_FC}}$, $\mathrm{SOC}_{\mathrm{min}}$, $P_{\mathrm{critical\_gen}}$, $\mathrm{SOC}_{\mathrm{stp\_gen}}$, $P_{\mathrm{critical\_FC}}$, $\mathrm{SOC}_{\mathrm{stp\_FC}}$, $\mathrm{H_2TANK_{stp}}$, $P_{\mathrm{lim\_charge}}$, $\mathrm{P1_{gen}}$, $\mathrm{P1_{FC}}$, and P2. All these control variables were explained in [14,15]. In some cases, some of these variables are not selected to be optimized because they are non-sense (for example, $P_{\mathrm{min\_gen}}$ will not be a control variable of the system if there is no diesel generator in the system) or because the user does not want to optimize them.

The secondary algorithm is a GA that searches for the best control strategy for each combination of components in the main algorithm. This GA is mono-objective (minimization of the costs). The GA uses an integer codification, using a vector in which the information concerning the control strategy is stored.

Codification of the control variables is done through a vector that consists of 12 positions, corresponding with the 12 control variables.

The fitness function of the combination i of the secondary algorithm is (rank 1 for the best individual, the one with lowest *NPC*, and rank N_{sec} for the worst solution):

$$\mathrm{fitness}_{\mathrm{SEC}_i} = \frac{(N_{\mathrm{sec}}+1) - i}{\sum_j [(N_{\mathrm{sec}}+1) - j]}, \qquad (19)$$

where N_{sec} is the number of solutions of the secondary algorithm, i is the rank of the solution of which its fitness is calculated, j are all the solutions of the main algorithm ($j = 1, \ldots, N_{\mathrm{sec}}$).

4.2.4. Steps of the algorithm

In this section, the algorithm that has been applied to perform the multi-objective design of the hybrid system is described.

In the following paragraphs, the steps taken to get the algorithm are indicated (see Fig. 3).

1. *Initialization of the population of the main algorithm.* In this first step, it is generated a random set of N_m possible solutions (or individuals) from the main algorithm (vectors codifying the combination of components), which will act as the initial population.
2. *Evaluate the secondary algorithm*. For each vector N_m of the main algorithm, the secondary algorithm is executed in order to find the best control strategy:
   a. N_{sec} vectors are obtained randomly from the secondary algorithm. These vectors have been described in Section 4.2.3, each one representing a possible control strategy.
   b. Each vector of the secondary algorithm together with the vector of the main algorithm codifies a hybrid system that is simulated and NPC is obtained. The secondary algorithm searches for the best control strategy to minimize NPC, so the N_{sec} vectors are evaluated by means of their aptitude (Eq. (19)).
   c. The best vectors (fittest) have a greater probability of reproducing themselves, crossing with other vectors. In each cross of two vectors, two new vectors are obtained (descendents). Descendents are then evaluated and the best of them replace the worst individuals of the previous generation (iteration).
   d. To find the optimal solution and not to stay in local minimal, some solutions randomly change some of their components (mutation).
   e. The individuals (vectors) obtained from reproduction and mutation are evaluated, making the next generation.

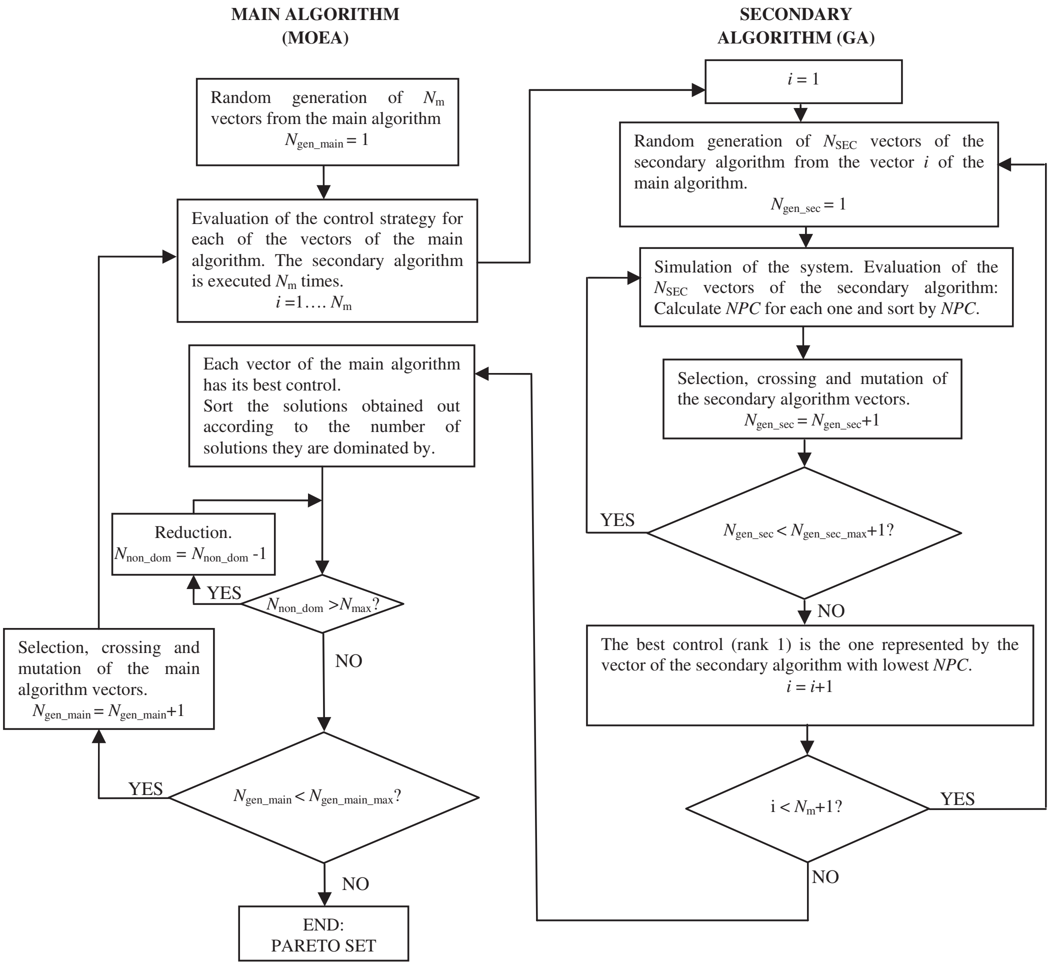

Fig. 3. Flowchart.

 f. The process continues (from 2.2 to 2.5) until a determined number of generations ($N_{gen\_sec\_max}$) have been evaluated, obtaining the optimal control strategy.

3. *Sorting out according to the number of solutions they are dominated by*. The vectors of the main algorithm are sorted out by the number of solutions they are dominated by (taking into account NPC, E and UL), calculating their fitness by Eq. (18).
4. *Reduction of the non-dominated Pareto set*. In order to prevent a number of non-dominated solutions (N_{non_dom}) similar to the number of solutions (N_m) (avoiding solutions too near each other in the Pareto set which does not contribute to variety), the program takes into account two inputs indicated by the user:
   a. The maximum NPC for the non-dominated solutions, in percentage over the minimum NPC of the non-dominated solutions, NPC_{over} (%). If a non-dominated solution has a NPC greater than the minimum NPC of the non-dominated solutions incremented by the percentage indicated by the designer (NPC_{over}), this solution is discarded.
   b. The maximum number of non-dominated solutions allowed (N_{max}). If the size of the non-dominated Pareto set is greater than the admissible maximum, as indicated by the designer (N_{max}), its size is reduced by means of the truncation technique. This reduction technique selects the solution, which has the minimum distance to another solution. The distance between two non-dominated solutions i and j is:

$$D_{i-j} = \sqrt{\left[\frac{NPC_i - NPC_j}{NPC_{max}}\right]^2 + \left[\frac{UL_i - UL_j}{UL_{max}}\right]^2 + \left[\frac{E_i - E_j}{E_{max}}\right]^2}, \quad (20)$$

   where NPC, UL, and E are, respectively, the total net present cost (€), the unmet load (kWh/year) and the total amount of kg of CO_2 produced by the hybrid system throughout one year (kg/year). The values denoted by "max" are the maximum values of the non-dominated solutions.
   After knowing the two solutions i and j that have the minimum D_{i-j}, the one is selected (i or j) that has the shortest distance to another solution in the set. With this reduction method, solutions at the extremes of the Pareto front will never be eliminated. This process is repeated as many times as required, eliminating solutions, until the size of the Pareto set drops to the value specified by the designer (N_{max}).
5. *Stopping criterion.* If the maximum number of generations indicated by the user ($N_{gen\_main\_max}$) has been reached, execution stops. Otherwise, selection, crossing and mutation will go on.
6. *Application of the selection, crossing and mutation operators*. The solutions that will participate in the single point crossing operator [27] are selected (selection operator) from this very

set using the roulette method. After crossing those solutions it is obtained a new population that will substitute the original. Finally, the mutation operator [27] is applied. Return to step 2.
7. *Solution selection.* At this point, there exists a set of solutions that defines the Pareto frontier of non-dominated solutions. Among them, the designer will select as the best solution the one that satisfies the associated objectives taken into account as well as other criteria, which are considered relevant (O&M costs, etc.).

5. Computational results: multi-objective optimization of a hybrid system

By using the developed program, a PV–wind–diesel–hydrogen–batteries system located in Zaragoza (latitude 41.65°), Spain, has been studied. The load profile considered is shown in Fig. 4 (AC load). The daily load profile is represented by a sequence of powers, each considered as constant over a time-step of 1 h.

The irradiation on horizontal surface and wind speed data at 10 m height are the average data for the last 10 years.

The system has a 48 V DC voltage and a 230 V AC voltage. The power factor of the AC load is $\cos\varphi = 0.9$. The wind speed hourly data (at 10 m height) and the irradiation in the area of the town are given by the average hourly values for the last few years.

The maximum unmet load allowed is 10% of the total annual load.

The nominal interest rate considered is 4% annually.

The annual general inflation rate is 3%. This rate is applied in order to calculate the cost of replacement of elements of the system when they reach the end of their own lifespan; it is also used to calculate the remaining value of the elements at the end of the lifetime of the system.

The nominal interest rate and the inflation considerably influence the value of the NPC of the system. To verify its effect on the NPC, several designs can be made using different values for these two parameters. Nevertheless, since only one objective (NPC) would be affected by modifying the nominal interest rate and the inflation, and a multi-objective design is realized, it has been decided to keep both values constant in all the design cases.

However, some elements have their own annual inflation rate, different from the general inflation rate (to be taken into account in order to estimate their cost when they finish their useful life and must be replaced).

The complete system lifespan estimated is 25 years.

The components considered in the optimization are explained in the following sections.

5.1. PV generators

PV generators (sets of PV panels in series and in parallel) have been considered instead of data for discrete panels, so the number of panels in parallel will always be one and this number will not be optimized. There are 12 possible different PV generators, shown in Table 1. Each hybrid system will include one of them. The panels have an inclination of 60° (in order to minimize the unmet load in winter time, because load in winter time is considered more important in this example), 0° azimuth and 0.2 albedo. Their lifespan is 25 years and the nominal voltage is 48 V DC. The loss factor F_{loss} considered is 1.2.

5.2. Wind turbines

There are six possible different wind generators, shown in Table 2. It has been considered that the number of wind generators must be one, so this number will not be optimized. The type of ground roughness considered is class 2.5 (0.2 m roughness length). The height above sea level is 247 m. The height of the hub is 10 m, the nominal voltage is 48 V DC and the lifespan is 20 years for all of the wind turbines considered.

In order to calculate the replacement cost (when the wind turbine has reached its lifespan), the annual inflation rate considered for wind turbines costs is −4% (these costs may be increased at a rate different from that of generic inflation figures, and in this case, it is expected that the prices will decrease a 4% annual) and the expected limit of the maximum variation of the wind turbines costs is −20% (this limit will be achieved in 4.4 years; after that, the wind turbines will be assumed to see their prices increased in line with general inflation).

5.3. Batteries

Battery banks (sets of batteries in series and in parallel) have been considered instead of data for discrete batteries, so the

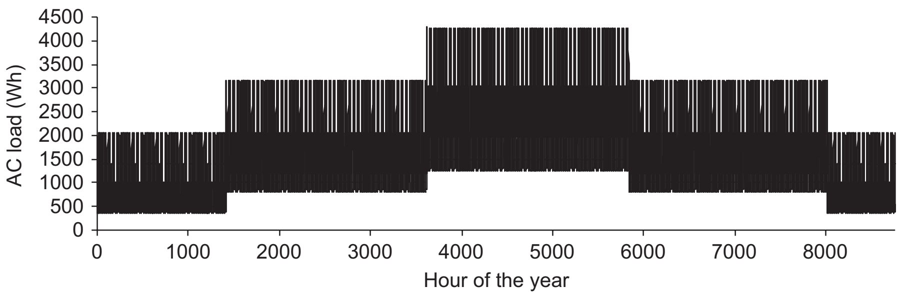

Fig. 4. Load (AC only).

Table 1
PV generators considered

Nominal peak power of the PV generator (kW_p)	0	0.5	1	1.5	2	2.5	3	4	5	6	7	8
Shortcut current (A)	0	7.6	15.2	22.8	30.4	38	45.6	60.8	76	91.2	106	122
O&M cost (€/year)	0	30	33	37	40	44	50	60	70	80	90	100
Acquisition cost (k€)	0	3	6	9	11.7	14.5	17	22	26	30	35	40

Table 2
Wind turbines

	Type					
	1	2	3	4	5	6
Maximum output power (W)	0	275	640	1760	3500	6500
Wind speed at maximum output power (m/s)	–	14	14	14	14	14
Output power (W) at 2 m/s	0	0	0	0	0	0
Output power (W) at 4 m/s	0	30	75	240	505	1000
Output power (W) at 6 m/s	0	75	180	600	1000	2000
Output power (W) at 8 m/s	0	150	350	1000	1900	3700
Output power (W) at 10 m/s	0	210	510	1260	2500	5000
Output power (W) at 12 m/s	0	250	605	1500	3100	6000
Output power (W) at 14 m/s	0	275	640	1760	3500	6500
Output power (W) at 16 m/s	0	215	525	1480	3000	5800
Output power (W) at 18 m/s	0	220	535	1540	3100	6000
Output power (W) at 20 m/s	0	230	550	1650	3300	6000
Output power (W) at ⩾22 m/s	0	0	0	0	0	0
O&M cost (€/yr)	0	50	50	50	55	60
Acquisition cost (€)	0	2273	3013	4114	6525	10,018

Table 3
Battery banks

Nominal capacity of the battery bank (Ah)	0	43	96	200	462	924	1848
Nominal capacity of the battery bank (kWh)	0	2.06	4.61	9.6	22.18	44.35	88.7
Maximum current (A)	–	7	12	24	51	102	204
Roundtrip efficiency (%)	–	80	80	80	80	80	80
O&M cost (€/year)	0	80	90	102	125	150	190
Acquisition cost (€)	0	620	1032	2260	4068	7600	14,400

number of batteries in parallel will be always one and this number will not be optimized. There are seven possible different battery banks, shown in Table 3. The minimum state of charge (SOC_{min}) recommended by the manufacturer for all of them is 30%, and the self-discharge coefficient is 3% monthly. It has been considered that all of them have 48 V DC nominal voltage and 12 years of floating life. All of them have the same curve of cycles to failure vs. depth of discharge (Fig. 2). The battery model considered is Ah model [18] and the lifespan for the batteries is estimated by the cycle count (Rainflow method), according to Downing's algorithm [22].

The annual inflation rate for battery banks costs considered is the same as the one considered for the wind turbines.

5.4. Diesel generators

There are six possible different diesel generators, shown in Table 4. The fuel (gas–oil) price is 1.2 €/l with 10% annual inflation rate. The expected CO_2 emissions are 2489 kg CO_2/l. Fuel consumption parameters considered are the same for all the diesel generators: $A = 0.246$ l/kWh and $B = 0.08145$ l/kWh [25].

The minimum output power recommended by the manufacturer is 30% of the rated power and the lifespan is 7000 h, for all the diesel generators considered.

5.5. Fuel cells

There are six possible different fuel cells, shown in Table 5. The minimum output power recommended by the manufacturer is 10% of the nominal power and the lifespan is 15,000 h for all of them.

The hydrogen consumption parameters considered are the same for all the fuel cells: $A_{FC} = 0.05$ kg/kWh, $B_{FC} = 0.004$ kg/kWh, $P_{max\_ef} = 0.2$, and $F_{ef} = 1$.

Table 4
Diesel AC generators

Rated output power (kVA)	0	1.9	3	4	5.5	7
O&M cost (€/h)	0	0.15	0.17	0.18	0.22	0.24
Acquisition cost (€)	0	1269	1514	1900	2314	2800

Table 5
Fuel cells

Nominal output power (kW)	0	1	2	3	4	5
O&M cost (€/h)	0	0.1	0.12	0.15	0.17	0.2
Acquisition cost (€)	0	7000	12,000	16,000	20,000	24,000

The annual inflation rate considered for wind turbines costs is −20% (these costs may be expected to increase at a rate different from that of generic inflation figures; in this case, it is expected that the prices will decrease at 20% annual) and the limit expected of the maximum variation of the hydrogen components costs is −60% (this limit will be achieved in 4.1 years; after then, the hydrogen components will be assumed to see their prices increased in line with general inflation).

5.6. Electrolyzers

There are seven possible different electrolyzers, shown in Table 6. The minimum input power is 10% of the nominal power and the lifespan is 10 years for all the electrolyzers considered.

The electrical consumption parameters considered are the same for all the electrolyzers: $A_E = 40$ kW/kg/h, $B_E = 20$ kW/kg/h.

Table 6
Electrolyzers

Nominal input power (kW)	0	1	2	3	4	5	6
O&M cost (€/year)	0	40	45	50	55	60	65
Acquisition cost (€)	0	7200	13,500	18,000	23,000	27,000	31,000

5.7. Inverters

There are five possible different inverters: 0, 2.2, 3.3, 4.5, and 5.5 kV A, with prices 0, 2300, 3200, 4300, and 5200 €, respectively. The lifespan is 10 years and the efficiency depends on the output power (maximum efficiency 92% at 20% output power).

5.8. Other data

The rectifier, the battery charge regulator and the hydrogen tank are selected at the end of the simulation of each combination of components and control variables.

The cost of the rectifiers is 200 €/kW, the lifetime is 10 years and the efficiency is 90%. The cost of the batteries charge regulator is 30+4 €/A and the lifetime is 10 years.

The specific cost of the hydrogen tank is 1000 €/kg, the maximum capacity allowed is 10 kg. The lifespan expected is 20 years and the annual O&M cost is 50 €/year.

5.9. Results

Several executions of the design program have been worked out, determining the best values of the parameters, evaluating convergence and computational time for the algorithms. The parameters used in this case are the following (they are entered by the user):

- *Main algorithm (MOEA):* number of generations $N_{gen\_main\_max} = 20$. Population $N_m = 300$. Maximum size of the Pareto front is $N_{max} = 50$. Crossing probability is 0.9. Mutation rate is 0.01. The maximum NPC for the non-dominated solutions is 60% over the lowest NPC of the non-dominated solution ($NPC_{over} = 60\%$).
  In this case, only seven of the 11 possible positions of the vector are optimized (Section 4.2.2): *b* (type of PV generator), *c* (type of wind turbine), *g* (type of battery bank), *h* (type of AC generator), *i* (type of fuel cell), *j* (type of electrolyzer) and *k* (type of inverter). Number of possible combinations of components is $12 \times 6 \times 7 \times 6 \times 6 \times 7 \times 5 = 635{,}040$.
  However, the number of combinations evaluated by the main algorithm is less than (number of generations · population) $20 \times 300 = 6000$.
- *Secondary algorithm (GA):* number of generations $N_{gen\_sec\_max} = 20$. Population $N_{sec} = 100$. Crossing probability is 0.9. Mutation rate is 0.01. The control variables to be optimized are 10: P_{min_gen}, P_{min_FC}, SOC_{min}, $P_{critical\_gen}$, SOC_{stp_gen}, H_2TANK_{stp}, P_{lim_charge}, $P1_{gen}$, $P1_{FC}$, and P2. Each variable can take five values, the number of combinations of the control strategy is $5^{10} = 9{,}765{,}625$.
  However, the number of combinations of the control strategy evaluated by the secondary algorithm is less than (number of generations × population) $20 \times 100 = 2000$.

With a Pentium IV 3.4 GHz, 1 GB RAM, about 50 evaluations per second can be performed. The number of combinations of components and control strategies is $635{,}040 \times 9{,}765{,}625 = 6.2 \times 10^{12}$. Evaluating all the combinations would take 3933 years. This fact demonstrates that an enumerative technique (classical technique) is not adequate to solve this kind of optimization problems.

GAs are suitable for this kind of problem because evaluating all the combinations is impossible. The number of combinations evaluated by the design tool, using GAs, is less than $6000 \times 2000 = 1.2 \times 10^7$. This task has taken 68 h.

The evolution of the 3D Pareto front can be observed in Fig. 5 (first and last Pareto fronts).

In Figs. 6–8, the different 2D representations of the last Pareto front (20th generation of the main algorithm) are shown.

There are 35 solutions in the Pareto set of the last generation. As an example, in Table 7, three solutions of the Pareto front can be observed in detail: solution 1, 9, and 31.

In Figs. 9–15, the hourly simulation through the year for solution 31 can be observed. Fig. 11 shows that the diesel generator starts working in June, when the load becomes higher. Hydrogen tank capacity in this case is the maximum allowed (10 kg). Fig. 12 shows that the hydrogen tank is full before March. In Fig. 14, it can be observed that, in March and April, there is excess energy, which could be stored in the hydrogen tank if the maximum hydrogen tank capacity allowed was higher.

However, it can be seen that storing energy in the hydrogen tank is much more inefficient than storing energy in batteries, so when the renewable sources produce more energy than is

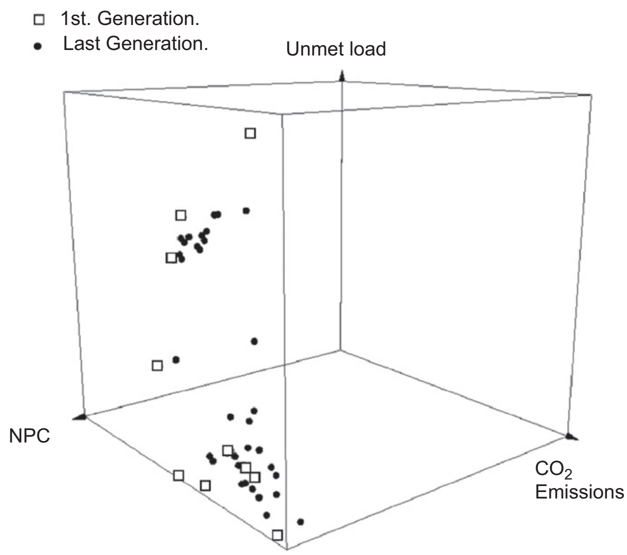

Fig. 5. 3D Pareto front for the first and the last generations.

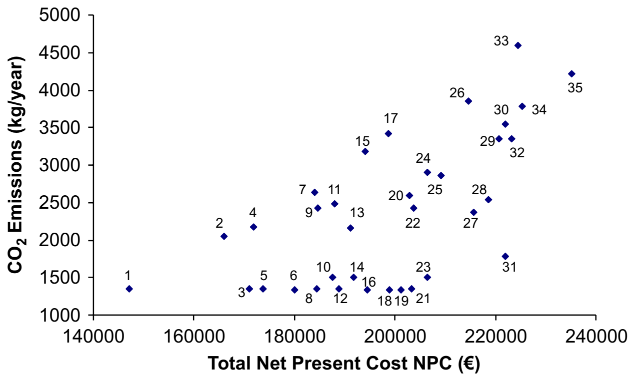

Fig. 6. 2D Pareto front for the last generation. CO_2 emissions vs. NPC.

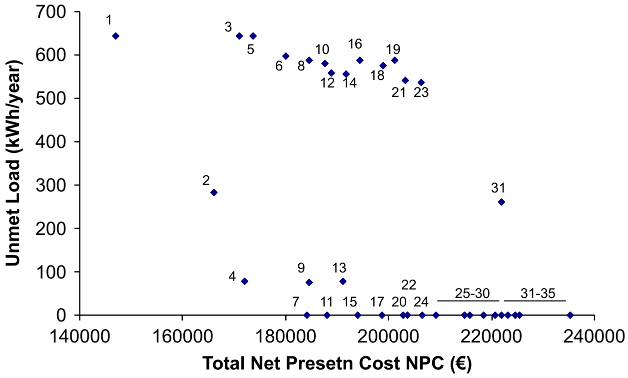

Fig. 7. 2D Pareto front for the last generation. Unmet load vs. NPC.

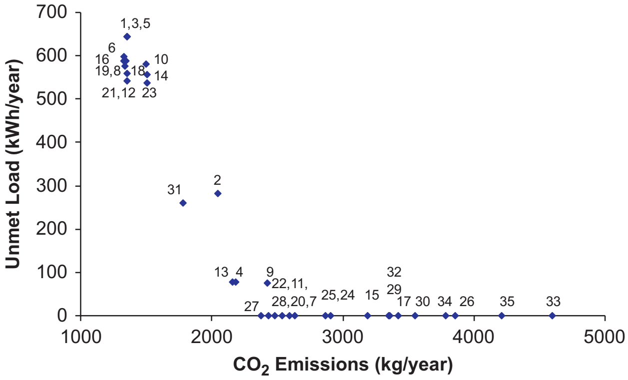

Fig. 8. 2D Pareto Front for the last generation. Unmet load vs. CO_2 emissions.

demanded, the surplus power is used to charge the batteries as much as possible and, if there is still more energy left, then this spare energy can also produce hydrogen in the electrolyzer ($P_{charge,}$ in solution 31, has a high value).

In Fig. 15, the unmet load is shown, being higher in summer. Unmet load in winter time is near 0, due to the step inclination of PV panels, among several other reasons.

6. Conclusions

In this paper, it has been applied, for the first time, the SPEA to the multi-objective design of hybrid systems of electrical energy generation, minimizing, simultaneously, three objectives: and cost, pollutant emissions unmet load.

The problem of design is very complex. The classical optimization techniques are not able to solve the problem of optimization consuming a reasonable CPU time. Nevertheless, the SPEA obtains a set of non-dominated solutions with little computational effort.

Compared with mono-objective methodologies of design [2–8], the design tool presented in this paper realizes a multi-objective design, obtaining the best solutions that the applied Evolutionary Algorithm has found, simultaneously considering three objectives. These solutions are non-dominated and they form the Pareto front. Each one is composed by a combination of physical components (photovoltaic generator, wind turbine, etc.), as well as the best strategy for controlling the system that it has been possible to find for this combination of elements. The designer can select the solution he/she considers most adequate from the set of solutions obtained, studying for each solution its NPC, the pollutant emissions and the unmet energy. Thus the designer can limit the acceptable maximum and minimal values for each objective, it being possible to select and study several solutions, which agree with the limits that have been imposed. Using a methodology of mono-objective design, it would not be

Table 7
Three solutions of the Pareto set (last generation)

	Solution 1	Solution 9	Solution 31
Peak power of the PV generator (kW_p)	8	8	8
Wind turbine	Type 6	Type 6	Type 6
Wind turbine peak power (kW)	6.5	6.5	6.5
Nominal capacity of battery bank (kWh)	88.7	44.3	88.7
Diesel generator rated power (kVA)	1.9	4	3
Electrolyzer nominal power (kW)	0	0	4
Fuel cell nominal power (kW)	0	0	3
Hydrogen tank capacity (kg)	0	0	10
Inverter nominal power (kVA)	5.5	5.5	5.5
Charge regulator current (A)	201	201	201
Rectifier power (kW)	83	678	495
Dispatch strategy:			
SOC_{min} (%)	30	30	40
P_{lim_charge} (W)	–	–	11,558
$P1_{gen}$ (W)	31,284	28,809	41,118
$P1_{FC}$ (W)	–	–	3903
P2 (W)	–	–	1819
Priority $P < P2$ (generator or fuel cell)	–	–	Generator
P_{min_gen} (VA)	570	1200	1200
P_{min_FC} (W)	–	–	700
$P_{critical\_gen}$ (W)	0	0	0
SOC_{stp_gen} (%)	30	30	30
H_2TANK_{stp} (kg)	0	0	0
Annual electrical energy delivered by PV generator (kWh/year)	8610	8610	8610
Annual electrical energy delivered by wind turbine (kWh/year)	8571	8571	8571
Annual battery through-output energy (kWh/year)	5714	5620	5764
Annual electrical energy consumed by electrolyzer (kWh/year)	–	–	951
Annual electrical energy delivered by fuel cell (kWh/year)	–	–	101
Annual overall load energy (kWh/year)	14,039	14,039	14,039
Annual excess energy (kWh/year)	1720	1962	742

Table 7 (*continued*)

	Solution 1	Solution 9	Solution 31
Batteries replacement cycle (year)	9.62	4.92	9.61
Annual hours of diesel operation	1241	1267	1157
Annual hours of electrolyzer operation	–	–	328
Annual hours of fuel cell operation	–	–	98
Unmet annual load (kWh/year)	644.1	74.8	257.8
Unmet load (%)	4.5	0.5	1.8
CO_2 emissions (kg CO_2/year)	1353	2421	1778
Total net present cost of the system (€)	147,026	184,571	221,945

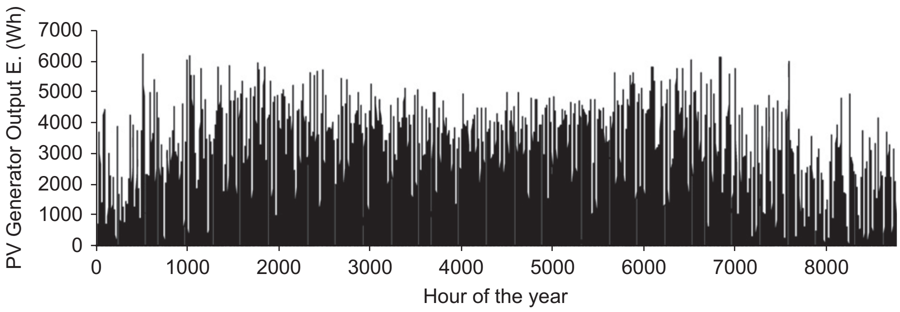

Fig. 9. PV generator output energy (solution 31).

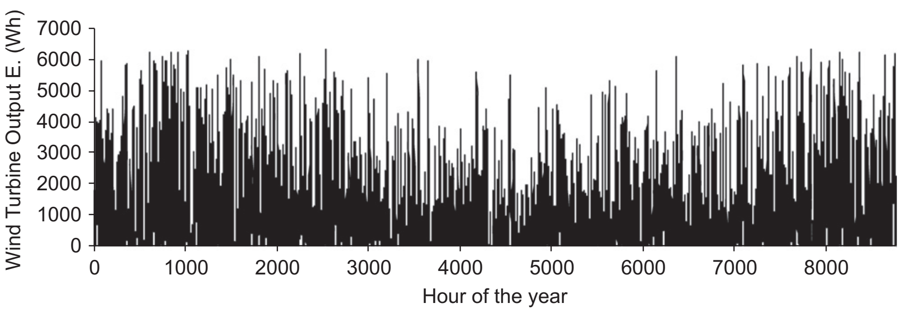

Fig. 10. Wind turbine output energy (solution 31).

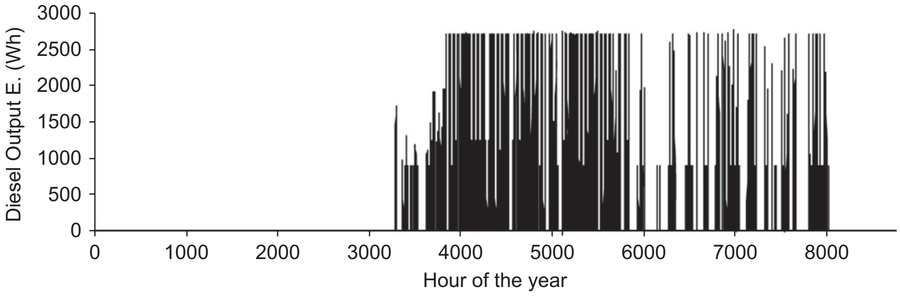

Fig. 11. Diesel generator output energy (solution 31).

possible to make this selection of solutions considering, in addition to the cost, the reliability and the pollutant emissions. An example of application has been explained, the design of a PV–wind–diesel–hydrogen–battery system in Zaragoza. The results state the practical value this method has for the designer, making it possible to select any of the solutions obtained by the algorithm. In the example shown, the Pareto front is formed by 35 solutions.

It is observed that many of the obtained solutions possess the wind turbine with the major power and the largest sized photovoltaic generator. The major power wind turbine and smaller photovoltaic generators have other solutions, because of

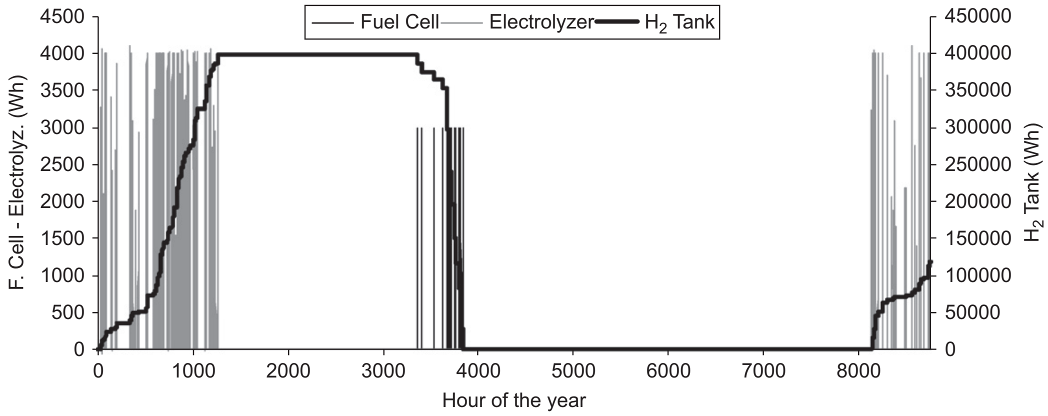

Fig. 12. Fuel cell output energy, electrolyzer input energy and H_2 tank stored energy (solution 31).

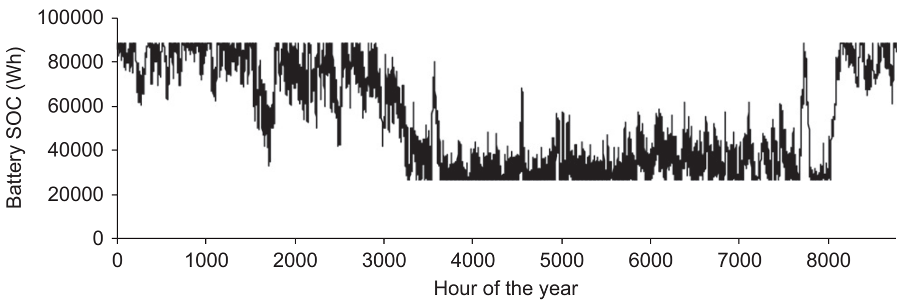

Fig. 13. Battery bank SOC (solution 31).

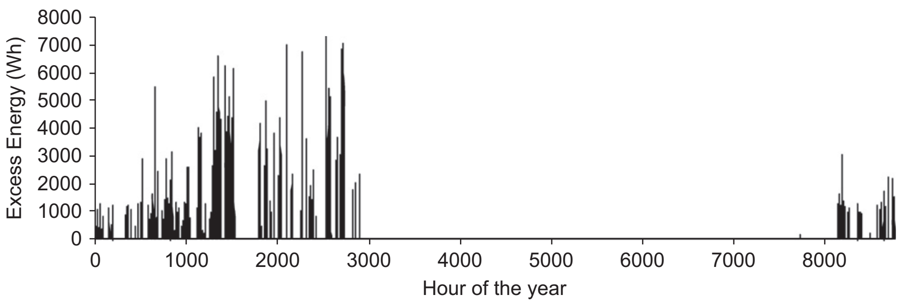

Fig. 14. Excess energy (solution 31).

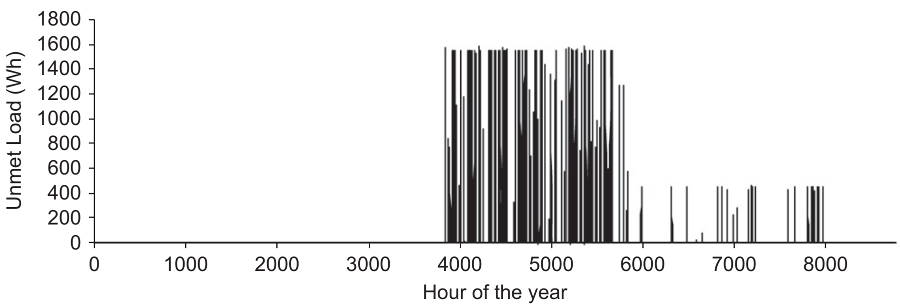

Fig. 15. Unmet load (solution 31).

the high cost of the photovoltaic panels. These configurations with high renewable fraction are due to the high wind potential in Zaragoza and also the high cost of diesel fuel (as well as to the high value of the specific inflation of diesel fuel).

Due to the high costs of the components of the hydrogen, energy storage in most solutions is done only using batteries. Some solutions incorporate storage in batteries and in hydrogen, but in these cases, the ideal control strategy gives priority to storage in batteries, as in case of solution no 31.

Acknowledgments

This work was supported by the "Ministerio de Educación y Ciencia" of the Spanish Government under Project ENE2006-14973/ALT and by the FEDER funds of the European Union.

References

[1] Collette Y, Siarry P. Multiobjective optimization: principles and case studies. 1st ed. Springer; 2004.
[2] Morgan TR, Marshall RH, Brinkworth BJ. 'ARES'—a redefined simulation program for the sizing and optimisation of autonomous hybrid energy systems. Sol Energy 1997;59(4–6):205–15.
[3] Seeling-Hochmuth GC. A combined optimisation concept for the design and operation strategy of hybrid-PV energy systems. Sol Energy 1997;61(2):77–87.
[4] McGowan JG, Manwell JF. Hybrid wind/PV/diesel system experiences. Renew Energy 1999;16(1–4):928–33.
[5] Muselli M, Notton G, Louche A. Design of hybrid-photovoltaic power generator, with optimization of energy management. Sol energy 1999;65(3):143–57.
[6] Elhadidy MA. Performance evaluation of hybrid (wind/solar/diesel) power systems. Renew Energy 2002;26(3):401–13.
[7] Dufo-López R, Bernal-Agustín JL. Design and control strategies of PV–diesel systems using genetic algorithms. Sol Energy 2005;79(1):33–46.
[8] Lund H, Duić N, Krajačić G, Carvalho MG. Two energy system analysis models: a comparison of methodologies and results. Energy 2007;32(6):948–54.
[9] Michalewicz Z, Fogel DB. How to solve it: modern heuristics. 2nd ed. Berlin: Springer; 2004.
[10] Coello CA, Veldhuizen DAV, Lamont GB. Evolutionary algorithms for solving multi-objective problems. New York: Kluwer Academic/Plenum Publishers; 2002.
[11] Zitzler E, Thiele L. Multiobjective evolutionary algorithms: a comparative case study and the strength Pareto approach. IEEE Trans Evol Comput 1999;3(4):257–71.
[12] Zitzler E, Laumanns M, Thiele L. SPEA 2: improving the strength pareto evolutionary algorithms. Technical report 103. Computer Engineering and Networks Laboratory, Swiss Federal Institute of Technology, Zurich, Switzerland, May 2001.
[13] Bernal-Agustín JL, Dufo-López R, Rivas-Ascaso DM. Design of isolated hybrid systems minimizing costs and pollutant emissions. Renew Energy 2006;31(14):2227–44.
[14] Dufo-López R, Bernal-Agustín JL, Contreras J. Optimization of control strategies for stand-alone renewable energy systems with hydrogen storage. Renew Energy 2007;32(7):1102–26.
[15] Dufo-López R. 2007. Dimensionado y control óptimos de sistemas híbridos aplicando algoritmos evolutivos (Design and control of hybrid systems using evolutionary algorithms). PhD thesis, Universidad de Zaragoza (University of Saragossa), April 2007.
[16] Rietveld M. A new method for estimating the regression coefficients in the formula relating solar radiation to sunshine. Agric Meteorol 1978;19:243–52.
[17] Graham VA, Hollands KGT. A method to generate synthetic hourly solar radiation globally. Sol Energy 1990;44(6):333–41.
[18] Schuhmacher J. INSEL—interactive simulation of renewable electrical energy supply systems, reference manual. University of Oldenburg, Renewable Energy Group, Deparment of Physics, 1993.
[19] Manwell JF, McGowan JG. A lead acid battery storage model for hybrid energy systems. Sol Energy 1993;50(5):399–405.
[20] Wenzl H, Baring-Gould I, Kaiser R, Liaw BY, Lundsager P, Manwell J, et al. Life prediction of batteries for selecting the technically most suitable and cost effective battery. J Power Sources 2005;144(2):373–84.
[21] HOMER "the hybrid optimization model for electric renewables". 〈http://www.nrel.gov/international/homer〉.
[22] Downing SA, Socie DF. Simple rainflow counting algorithms. Int J Fatigue 1982;4(1):31–40.
[23] Green HJ, Manwell J. HYBRID2—a versatile model of the performance of hybrid power systems. In: Proceedings of the WindPower'95, Washington, DC, 1995. p. 437–46.
[24] Manwell JF, McGowan JG, Rogers AL. Wind energy explained. New York: Wiley; 2002.
[25] Skarstein O, Ulhen K. Design considerations with respect to long-term diesel saving in wind/diesel plants. Wind Eng 1989;13(2):72–87.
[26] Sonntag RE, Borgnakke C, Wylen GJV. Fundamentals of thermodynamics. 6th ed. New York: Wiley; 2002.
[27] Bäck T, Fogel DB, Michalewicz Z. Evolutionary computation 1: basic algorithms and operators. Bristol and Philadelphia: Institute of Physics Publishing; 2000.